Hydromorphodynamic effects of the width ratio and local tributary widening on discordant confluences

S. Guillén-Ludeña[a,b,*], M.J. Franca[b], F. Alegria[c], A.J. Schleiss[b], A.H. Cardoso[a]

[a] CERIS, Instituto Superior Técnico, Universidade de Lisboa, Portugal
[b] Laboratory of Hydraulic Constructions, École Polytechnique Fédérale de Lausanne, Switzerland
[c] Instituto de Telecomunicaçoes, Instituto Superior Técnico, Universidade de Lisboa, Portugal

ARTICLE INFO

ABSTRACT

River training works performed in the last couple of centuries constrained the natural dynamics of channel networks in locations that include the confluences between tributaries and main channels. As a result, the dynamics of these confluences are currently characterized by homogeneous flow depths, flow velocities, and morphologic conditions, which are associated with impoverished ecosystems. The widening of river reaches is seen as a useful measure for river restoration, as it enhances the heterogeneity in flow depths, flow velocities, sediment transport, and bed substrates. The purpose of this study is to analyze the effects of local widening of the tributary mouth as well as the effects of the ratio between the width of the tributary and that of the main channel on the flow dynamics and bed morphology of river confluences. For that purpose, 12 experiments were conducted in a 70° laboratory confluence. In these experiments, three unit-discharge ratios were tested ($q_r = 0.37$, 0.50, and 0.77) with two width ratios and two tributary configurations. The unit-discharge ratio is defined as the unit discharge in the tributary divided by that of the main channel, measured upstream of the confluence. The width ratio, which is defined as the width of the tributary divided by that of the main channel, was modified by changing the width of the main channel from 0.50 to 1.00 m (corresponding to $B_r = 0.30$ and 0.15 respectively). The tributary configurations consisted of (i) a straight reach with a constant width (the so-called *reference configuration*) and (ii) a straight reach with a local widening at the downstream end (the so-called *widened configuration*). During the experiments, a uniform sediment mixture was continuously supplied to both channels. This experimental setup is novel among existing experimental studies on confluence dynamics, as it addresses new confluence configurations and includes a continuous sediment supply to both channels. The experiments were run until the outgoing sediment rate was nearly the same as the incoming; i.e., equilibrium had been achieved. The bed topography and water surface were then recorded in both channels. The results reveal that the width ratio and the locally widened tributary reach influence the dynamics of the confluence. The different width ratios influenced the size of the bank-attached bar at equilibrium, which was wider and longer for $B_r = 0.15$ than for $B_r = 0.30$. Other morphological differences were observed at equilibrium for the different width ratios, such as deeper scour holes and increased penetration of the tributary into the main channel. These differences were attributed to the different values of the ratio between the unit momentum-flux of the tributary and that of the main channel that were noted at equilibrium for the different width ratios. The local widening of the downstream reach of the tributary significantly enhanced the heterogeneity in flow depth, flow velocity, and bed morphology within the widened reach. This heterogeneity contrasts with the homogeneity observed in the tributary without widening (reference configuration). Additionally, the effects of the local tributary widening were limited to the tributary, with minor or negligible effects on the main channel.

1. Introduction

River confluences constitute the nodes of fluvial networks, as it is through the confluence of tributaries with main rivers that the most affluence of water and sediments is delivered to the main watercourses.

Additionally, from an environmental point of view, river confluences are considered to be strategic locations that enhance the fluvial ecosystem by providing ecological connectivity and diversity in flow, water quality, and sediment transport (Benda et al., 2004; Rice et al., 2006, 2008; Leite Ribeiro et al., 2012b). In anthropized rivers, confluences
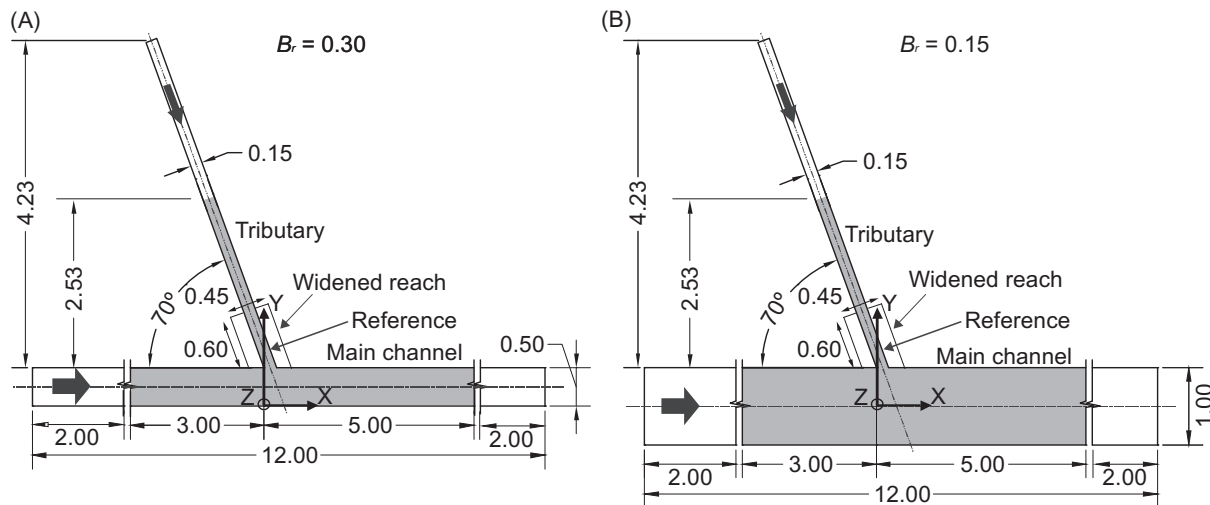
Fig. 1. Sketch of the laboratory confluence for (A) B_r = 0.30 and (B) B_r = 0.15. The shaded area indicates the measurement domain. Dimensions are in meters.
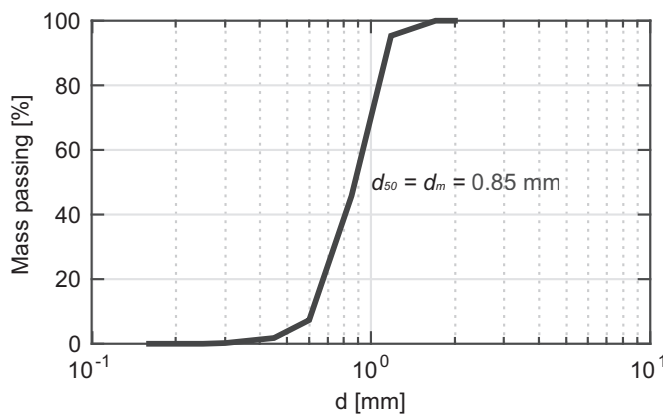

Fig. 2. Grain size distribution of the supplied sediment mixture.

may be seen as reset points in the landscape, which contribute to the reestablishment of pristine conditions in rivers (Moyle and Mount, 2007).

This study is inspired by mountain river confluences in general and by the confluences of the upper Rhone River basin in particular, which contain impoverished ecosystems owing to previous channelization works. These river training works have resulted in highly channelized tributaries that are environmentally disconnected from the main river by artificial ramps or weirs. At present, these confluences are characterized by homogeneous flow and morphologic conditions that negatively impact the natural dynamics of the confluences (Peter, 2006; Fette et al., 2007).
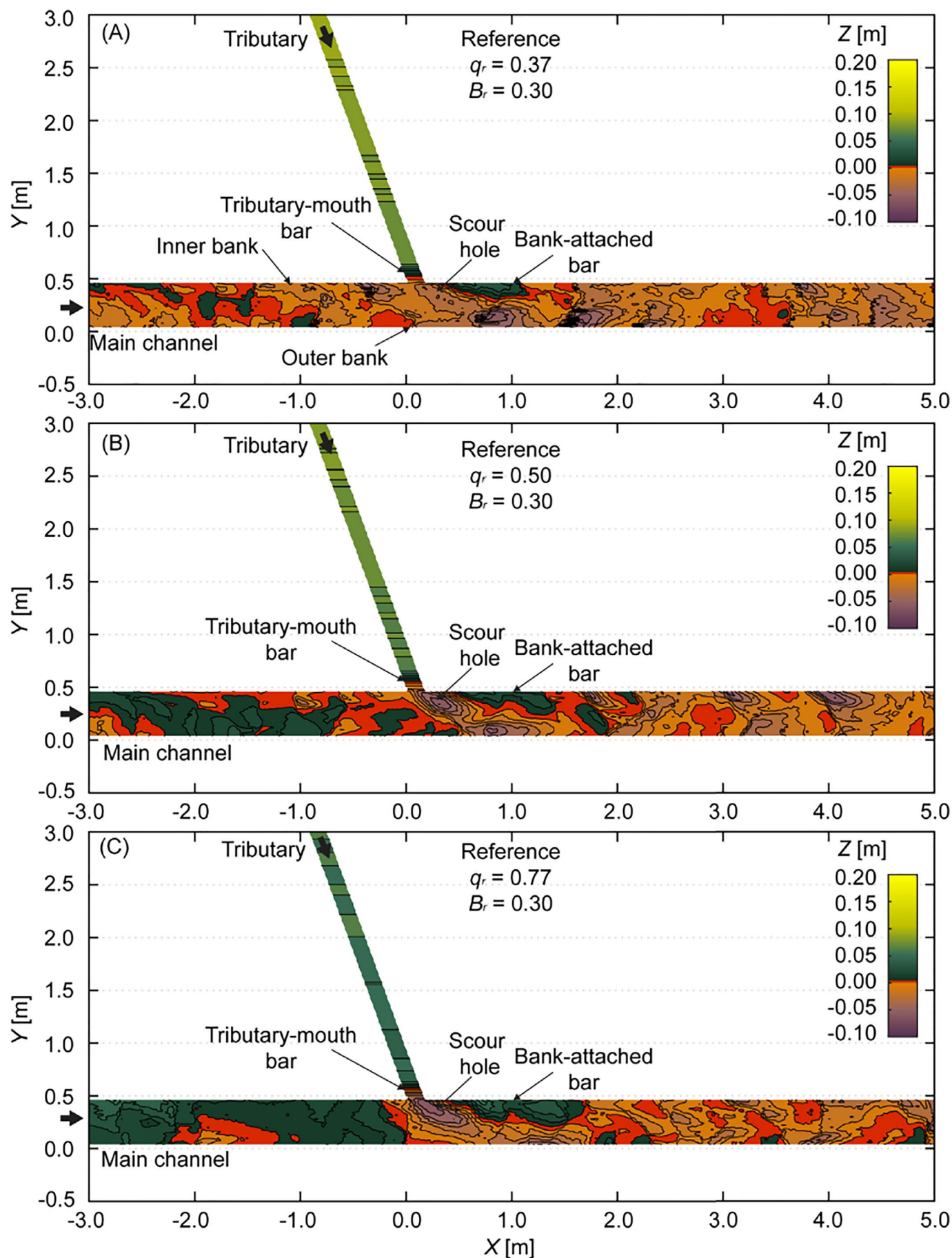
One of the most common measures in river restoration is the widening of river reaches (Bernhardt, 2005; Reichert et al., 2007). The aim of this widening is to recover the vital space required by rivers, to maintain the quantity and quality of water, and to enhance the heterogeneity in flow dynamics and bed morphology in the fluvial ecosystem (Nakamura et al., 2006; Sloff et al., 2006; Weber et al., 2009).

The success of river restoration projects depends on an understanding of the hydrodynamic, morphodynamic, and sedimentary processes involved in the dynamics of confluences (Bernhardt et al., 2007; Palmer et al., 2010). According to Mosley (1976), Best (1987, 1988), Biron et al. (1993), Rhoads (2006), and Best and Rhoads (2008), these processes are governed by parameters such as the junction angle, the width ratio, the flow and sediment discharges, the momentum-flux, and the bed material. Although these studies provide very valuable insights into the dynamics of river confluences; they cannot explain the hydromorphodynamic processes involved in mountain river confluences

completely, as they focus on confluences with higher discharge and width ratios than, for instance, those of the upper Rhone River basin (Leite Ribeiro et al., 2012b). In this study, the unit-discharge ratio, the momentum-flux ratio, and the width ratio are defined as the magnitude of the appropriate variable in the tributary divided by the corresponding value for the main channel; here, both of these values are measured upstream of the confluence.

The dynamics of mountain river confluences were studied by means of systematic laboratory experiments by Leite Ribeiro et al. (2012a, 2012b, 2016) and Guillén-Ludeña et al. (2015, 2016). They observed that these confluences are characterized by narrow and steep tributaries that convey substantial sediment loads, whereas the main channel provides the dominant flow discharge. These conditions typically result in low discharge and width ratios (Q_r < 0.5 and B_r < 0.3 respectively) and in a marked bed discordance between the tributary and main channel, which strongly influences the dynamics of the confluence (Biron et al., 1996; Boyer et al., 2006; Guillén Ludeña et al., 2017). Guillén-Ludeña et al. (2016) also reported different flow regimes in the tributary for different junction angles. Leite Ribeiro et al. (2012b, 2016), who fed sediments only to the tributary in their experiments, analyzed the effects of local tributary widening on the dynamics of a confluence with an angle of 90°. They concluded that the hydromorphodynamics in the widened reach were characterized by heterogeneity in flow depth, flow velocity, and bed morphology. In addition, Leite Ribeiro et al. (2012b, 2016) observed that local tributary widening did not provoke backwater effects in the tributary or in the main channel. Despite the great contribution of these studies to the understanding of the dynamics of mountain river confluences, they cover only a limited number of configurations, i.e., three discharge ratios (Q_r = 0.11, 0.15, and 0.23), two junction angles (α = 70° and 90°), a single width ratio (B_r = 0.30), and nonuniform sediment mixtures that resulted in armored beds (Leite Ribeiro et al., 2012b, 2016; Guillén-Ludeña et al., 2015, 2016). Moreover, in the case of Leite Ribeiro et al. (2012b, 2016), the absence of sediment supply to the main channel during their experiments led to bed armoring in the main channel, which hindered the development of a scour hole (Guillén-Ludeña et al., 2015).

The present study aims to analyze the effects of the width ratio and the local widening of the tributary mouth on the hydromorphodynamics of mountain river confluences. For that purpose, 12 experiments were conducted in a laboratory confluence in which three unit discharge ratios were tested (q_r = 0.37, 0.50, and 0.77). Each unit-discharge ratio was run with two width ratios (B_r = 0.30 and 0.15) and two tributary configurations (the reference and widened configurations). The adopted unit-discharge ratios (q_r) are equivalent to those

Fig. 3. Bed topography of the tributary and main channel at equilibrium for the experiments performed with $B_r = 0.30$ and with the reference (not widened) configuration for the tributary. Each frame corresponds to a different q_r value: (A) $q_r = 0.37$, (B) $q_r = 0.50$, and (C) $q_r = 0.77$. The bed elevation contours are spaced by $\Delta Z = 0.01$ m.

discharge ratios (Q_r) adopted by Leite Ribeiro et al. (2012a, 2012b, 2016) and Guillén-Ludeña et al. (2015, 2016). To avoid bed armoring, a uniform sediment mixture was continuously supplied to both channels during the experiments. This experimental setup complements those of Leite Ribeiro et al. (2012a, 2012b, 2016) and Guillén-Ludeña et al. (2015, 2016), as it covers new confluence configurations by analyzing two width ratios, studying the effect of tributary widening with a junction angle of 70°, and by continuously supplying a uniform sediment mixture to both channels.

The analysis performed in this study seeks to answer the following questions:

- Can local tributary widening enhance the heterogeneity in flow dynamics and bed morphology of confluences?
- Are the effects of local tributary widening limited to the widened reach, or do they also influence the rest of the tributary and/or the main channel?
- Do the dynamics of the tributary change when the width of the main channel is changed?

2. Experimental setup

2.1. Experimental facility

The experiments were carried out in a laboratory confluence at the Instituto Superior Técnico of the University of Lisbon (IST-UL). The confluence consisted of a 12-m-long, 1-m-wide, rectangular, straight main channel and a 5.9-m-long, 0.15-m-wide, rectangular, straight tributary that joined the main channel at an angle of 70° (Fig. 1). In this laboratory confluence, four geometries were tested that combined two width ratios ($B_r = 0.30$ and 0.15) with two geometries for the tributary. The width ratio was modified by changing the width of the main channel (Fig. 1). The tributary geometries consisted of

- one reference configuration formed by a tributary with a constant width of $B_t = 0.15$ m (Fig. 1); and
- one widened configuration in which the width of the downstream end of the tributary was increased from 0.15 to 0.45 m over a length of 0.60 m (Fig. 1).

2.2. Experimental parameters

Three unit-discharge ratios were tested for each tributary configuration and for each width ratio. Twelve experiments were conducted in total.

The unit discharge upstream of the confluence was kept the same for both width ratios. Hence, the flow discharge supplied to the main channel for $B_r = 0.15$ was twice as large as that supplied to the channel when $B_r = 0.30$.

A constant flow depth of 0.10 m was maintained at the downstream end of the main channel in all the experiments. This flow depth was adjusted using a tailgate installed at the downstream end of the main channel.

The sediment mixture supplied to the tributary and the main channel during the experiments consisted of sand with a grain size ranging from 0.4 to 2.0 mm. Fig. 2 shows the grain size distribution of the sediment mixture.

The sediment supply rates for the tributary (Q_{st}) and the main channel (Q_{sm}) were first estimated by using the sediment transport formula of Smart (1984) and by assuming equilibrium slopes of 0.3% for the main channel and 1% for the tributary. These slope values correspond to slopes observed at confluences in the upper Rhone River

basin (Guillén-Ludeña, 2015). Based on this procedure, the sediment transport rates supplied to the main channel (Q_{sm}) were 0.3 kg/min for $B_r = 0.30$ and 0.6 kg/min for $B_r = 0.15$; thus, the same sediment supply rate per unit width was maintained for the different width ratios. The sediment supply rate (Q_{st}) in the tributary was fixed at 0.5 kg/min in all experiments.

2.3. Procedure and measurements

First, the initial movable bed was prepared by using the sediment mixture that was subsequently supplied to both flumes. The bed in the main channel was initially almost horizontal, whereas a mild slope of ∼0.5% and a small bed discordance of ∼0.03 m were imposed on the tributary bed in order to accelerate the bed evolution toward equilibrium. These initial conditions did not appear to influence bed morphology and flow dynamics at equilibrium, as observed in previous experiments performed by the authors (Guillén-Ludeña et al., 2015, 2016).

The experiments were run until equilibrium was reached, meaning that the outgoing and the incoming sediment rates were nearly equal. This was evaluated by periodic weighing of the sediments trapped at the downstream end of the main channel.

Once equilibrium had been achieved, the water surface was recorded in the tributary and in the main channel by an ultrasonic limnimeter with an accuracy of ± 1 mm. A total of 22 longitudinal profiles with a lateral spacing of 0.02 m when $B_r = 0.30$ and were recorded in the main channel; a lateral spacing of 0.04 m was used when $B_r = 0.15$. Only one longitudinal profile along the channel axis was recorded in the tributary for the reference configuration, whereas nine longitudinal profiles with 0.05 m lateral spacing were recorded in the widened configuration. The spatial resolution of each longitudinal profile was 0.01 m for all measurements.

The same spatial grid was used to measure the bed topography at equilibrium. These measurements were performed with a Mini-Echo-Sounder with an accuracy of ± 1 mm.

3. Results

3.1. Bed morphology in the main channel

The morphodynamic features in the main channel at equilibrium were similar in all experiments. They included (i) a bank-attached bar that extended along the inner bank of the main channel downstream of the confluence, and (ii) a scour hole that extended from the tributary mouth to the outer bank of the main channel flanking the bar. These features are illustrated in Figs. 3–6, which show the bed topography at equilibrium for all experiments. Figs. 3 and 4 correspond to the three tested unit-discharge when $B_r = 0.30$ for the reference and widened configurations respectively. Figs. 5 and 6 show the bed topography in the experiments with $B_r = 0.15$ for the reference and widened configurations respectively.

Table 1 contains the dimensions of the morphological features in the main channel. The bank-attached bar is characterized in terms of its maximum height (H), length (L), maximum width (W), width-to-length ratio (W/L), and the ratio between the width of the bar and the width of the main channel (W/B_m). The scour hole at the tributary mouth is characterized in terms of its maximum depth (D).

The length and width of the bank-attached bar in the main channel and the ratio W/B_m increased with the increase in the unit-discharge ratio (Table 1). The height of the bar also increased with the unit discharge ratio, but only in the case of $B_r = 0.30$ for the reference configuration and in the case of $B_r = 0.15$ for the widened configuration.
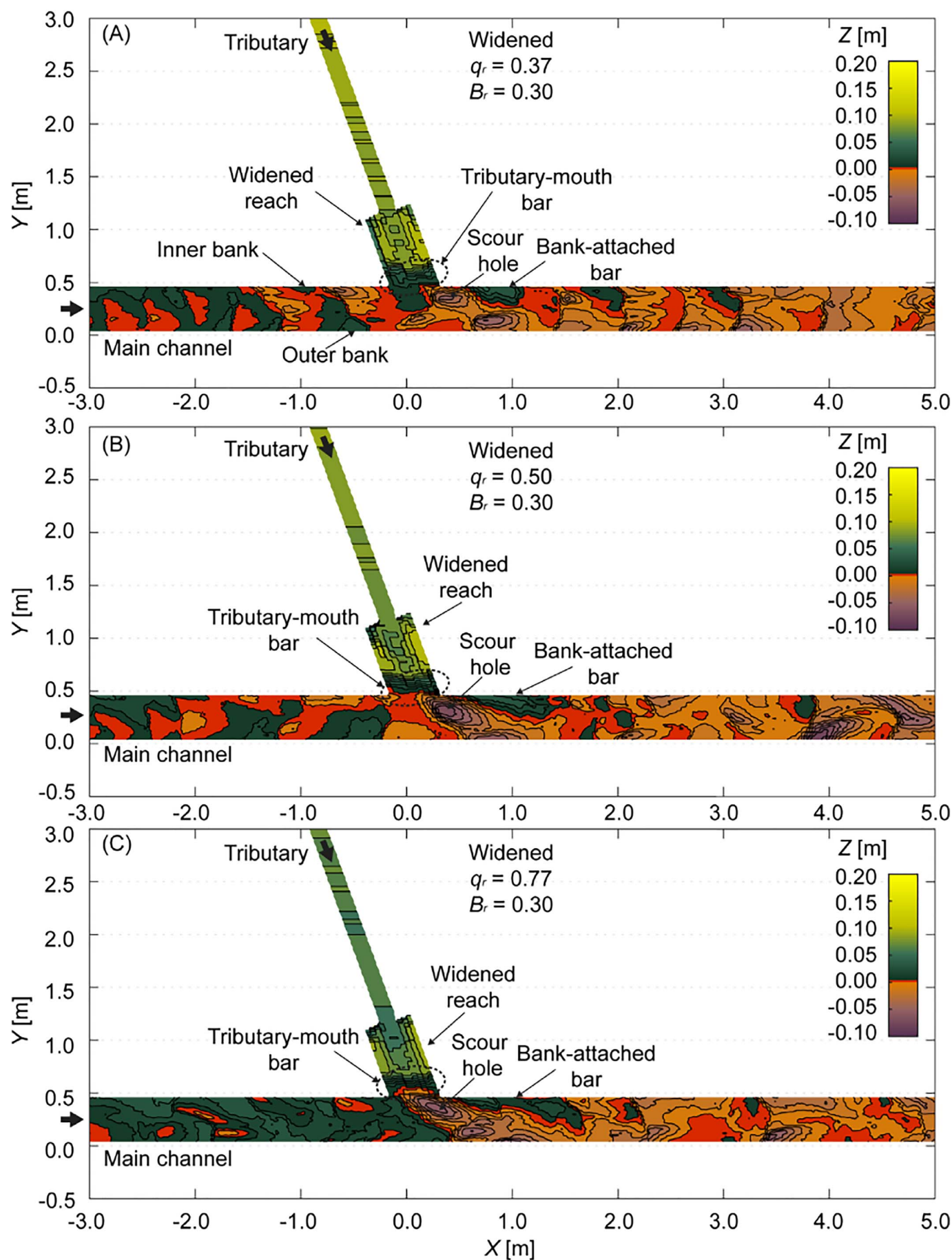
(caption on next page)

Fig. 4. Bed topography of the tributary and main channel at equilibrium for the experiments performed with $B_r = 0.30$ and with the widened configuration in the tributary. Each frame corresponds to a different q_r value: (A) $q_r = 0.37$, (B) $q_r = 0.50$, and (C) $q_r = 0.77$. The bed elevation contours are spaced by $\Delta Z = 0.01$ m.

The width and length of the bank-attached bar were significantly larger for $B_r = 0.15$ than for $B_r = 0.30$. However, the ratio W/B_m, which was also higher for $B_r = 0.15$ than for $B_r = 0.30$, displayed minor differences between the two width ratios, compared to the large differences observed for the width and length of the bar. Additionally, the width to length ratio of the bank-attached bar was nearly the same for all experiments and ranged from 0.19 to 0.23 (W/L in Table 1).

The depth of the scour hole at the tributary mouth increased with the unit-discharge ratio only in the experiments performed with the reference configuration (D in Table 1). Additionally, in the experiments performed with the reference configuration, the scour hole was deeper for $B_r = 0.15$ than for $B_r = 0.30$ for the high unit discharge ratio ($q_r = 0.77$). On the other hand, for the low and intermediate unit discharge ratios ($q_r = 0.37$ and 0.50, respectively), the depth of the scour hole was similar for both width ratios. In contrast, the experiments performed with the widened configuration showed that the depth of the scour at the tributary mouth was independent of the unit-discharge ratio (D in Table 1).

3.2. Hydrodynamics of the main channel

The following hydrodynamic features were observed at equilibrium in all experiments in the main channel: (i) a zone of flow deflection caused by the tributary inflow, (ii) a zone of low velocities in the vicinity of the downstream junction corner, (iii) a zone of flow acceleration downstream of the confluence, and (iv) a shear layer that extended from the tributary mouth to the middle of the post-confluence channel and surrounded the zone of reduced flow velocities. This shear layer separates the flow originating in the tributary from that coming from the main channel (Fig. 7). In addition to these features, in the experiments performed with the reference configuration, a zone of flow stagnation with near-zero velocities that was associated with a local rise in the water surface seemed to occur at the upstream junction corner (Fig. 7A). In the case of the experiments performed with the widened configuration, a zone of flow recirculation was observed at the upstream junction corner (Fig. 7C–D).

The features mentioned above are illustrated in Fig. 7, which illustrates the water surface and the flow under equilibrium conditions using dye that was injected into the tributary. The frames correspond to the four experiments performed with $q_r = 0.50$. These observations are also valid for the other unit-discharge ratios.

In the experiments performed with the widened configuration, the tributary inflow was deflected toward the downstream junction corner before it entered the main channel. In contrast, in the experiments performed with the reference configuration, the tributary inflow occupied the entire tributary width before entering the main channel (Fig. 7).

Table 2 contains the values of the spatially averaged flow depth (h), flow velocity (U), and Froude number (Fr) that correspond to the main channel upstream and downstream of the confluence (referred to using the indices *up* and *dw*, respectively). The average flow depth (h) is the spatial average of the local flow depths measured upstream of the confluence for $X < 0$ m and $Y < 0.5$ m and downstream of the confluence for $X > 0$ m and $Y < 0.5$ m. The average flow velocity (U) and the average Froude number (Fr) were obtained using the following equations.

$$U = \frac{Q}{B_m h} \tag{1}$$

$$Fr = \frac{U}{\sqrt{gh}} \tag{2}$$

where g is the gravitational acceleration.

As the unit-discharge ratio increased, the average flow depth measured upstream of the confluence (h_{up}) decreased. In contrast, the average flow depth measured downstream of the confluence (h_{dw}) did not show any pattern as the unit-discharge ratio increased. A convective flow acceleration was observed in the downstream direction in all experiments ($U_{dw} > U_{up}$ in Table 2). The flow velocities measured for $B_r = 0.30$ were larger than those measured for $B_r = 0.15$. The Froude number was larger in the downstream reach in all experiments. Additionally, for each unit-discharge ratio, the Froude number was larger for $B_r = 0.30$ than for $B_r = 0.15$.

3.3. Tributary

The bed morphology in the tributary displayed two common features for both tributary configurations and both width ratios. These features consisted of (i) a constant bed slope upstream of the confluence for $Y > 1.2$ m and (ii) a marked bed discordance between the tributary and the main channel that was formed by the so-called *tributary-mouth bar* (Best and Rhoads, 2008), the toe of which barely penetrated into the main channel. These features are illustrated in Fig. 8, which shows the bed elevation and water surface profiles along the tributary axis for each experiment.

The bed elevation and the slopes of the bed and water surface were similar for the experiments performed with the same unit discharge ratio, regardless of the width ratio and the tributary configuration (Fig. 8). Increasing unit discharge ratios resulted in a lower bed elevation of the tributary and thus in lower bed discordance. Additionally, the slopes of the bed and water surface decreased as the unit discharge ratio increased. The tributary-mouth bar penetrated farther into the main channel in the experiments performed with the widened configuration, compared to those performed with the reference configuration. The bed rise observed at the tributary mouth is a typical feature of the widened configuration that is analyzed later.

Constant flow depths were observed where $Y > 1.0$ m for the reference configuration and where $Y > 1.2$ m for the widened configuration (Fig. 8 and Table 3). These observations indicate quasi-uniform flow within these reaches.

Table 3 contains the values of the spatially averaged values of flow depth (h), flow velocity (U), and the Froude number (Fr), measured and averaged for $Y > 1.0$ m for the reference configuration and for $Y > 1.2$ m for the widened configuration.

Table 3 shows that for both tributary configurations and both width ratios the flow depth and the flow velocity increased with the unit-discharge ratio. In the experiments performed with $B_r = 0.30$, the flow velocity was lower than in the experiments performed with $B_r = 0.15$. The Froude number was also lower for $B_r = 0.30$ than for $B_r = 0.15$, particularly when the experiments performed with the reference configuration are compared. Moreover, the Froude number was higher for the experiments performed with the widened configuration, compared to those obtained for the reference configuration.

3.4. Widened reach

Flow visualizations using dye injected upstream in the tributary revealed the presence of the following hydrodynamic features in the widened reach of the tributary: (i) a central main flow corridor that was deflected to the downstream junction corner by the influence of the main channel flow, (ii) two recirculation zones flanking the main flow corridor, (iii) two shear layers that separated the recirculation zones from the main flow corridor, and (iv) two stagnation zones located at both upstream corners of the widened reach. These features are illustrated in Fig. 9, which shows a planview of the widened reach at two
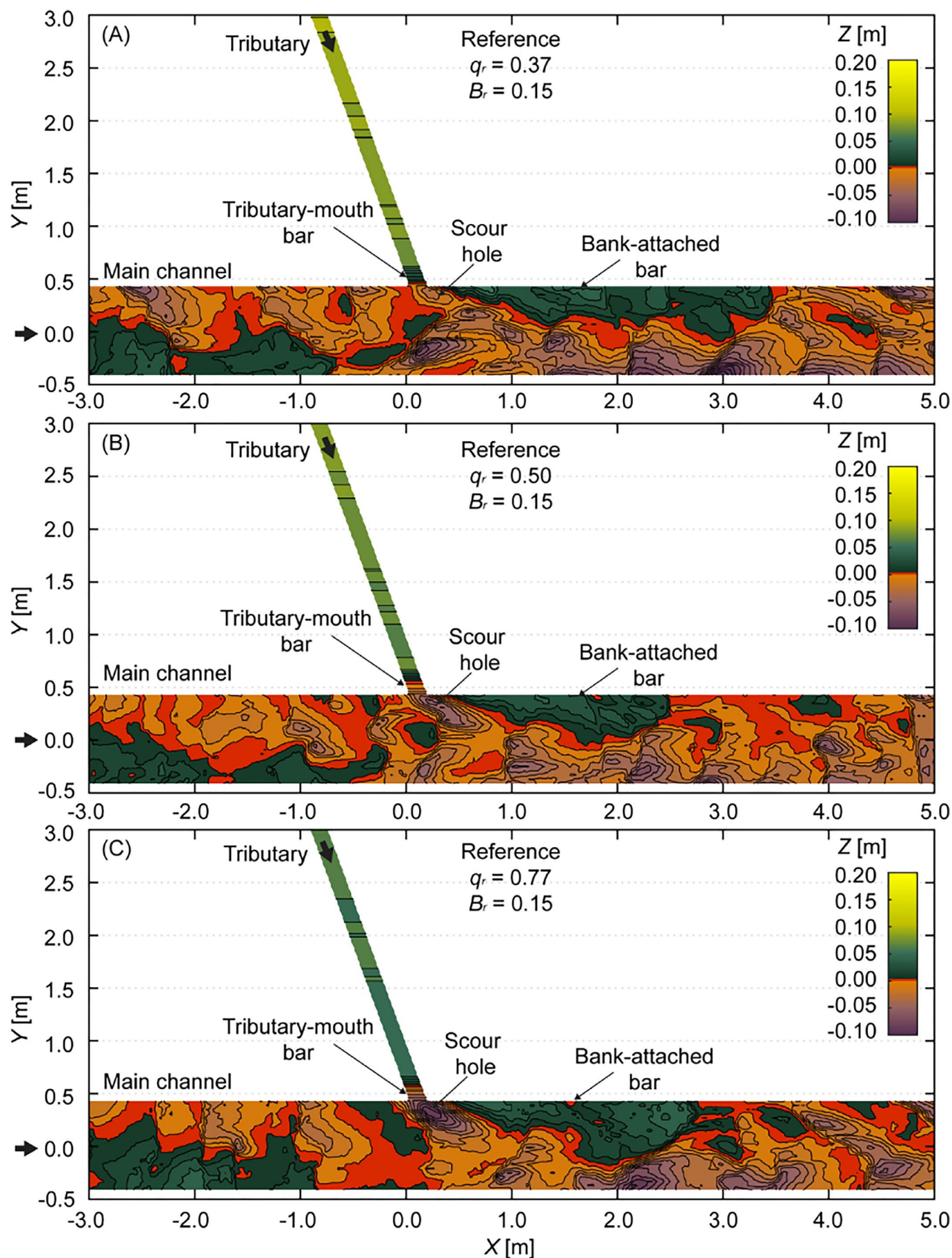
(caption on next page)

Fig. 5. Bed topography of the tributary and main channel at equilibrium for the experiments performed with $B_r = 0.15$ and with the reference (not widened) configuration in the tributary. Each frame corresponds to a different q_r value: (A) $q_r = 0.37$, (B) $q_r = 0.50$, and (C) $q_r = 0.77$. The bed elevation contours are spaced by $\Delta Z = 0.01$ m.

consecutive instants. The absence of dye in the recirculation zone located at the upstream bank indicates that this zone was fed primarily by flow from the main channel by means of the recirculation zone observed at the upstream junction corner. In contrast, the recirculation zone at the downstream bank of the widened reach was fed by the flow originating from the tributary, which was recirculated in the vicinity of the downstream junction corner.

The bed morphology of the widened reach was characterized by (i) a rise in the bed along the main flow corridor (Fig. 8) and (ii) zones of sedimentation along either bank of the widened reach that coincide with the recirculation zones. These features are illustrated in Fig. 10, which shows a view of the final topography of the tributary mouth from the downstream end of the tributary for both tributary configurations.

Fig. 11 depicts a detailed planview of the bed topography of the confluence for the six experiments performed with the widened configuration. Additionally, Fig. 12 depicts the bed elevation and water surface variations in the two cross sections indicated in Fig. 11A, i.e., cross sections I-I and II-II.

In the widened configuration, the front of the tributary-mouth bar was eroded in the vicinity of the upstream junction corner by the flow recirculation observed therein (Fig. 7C–D). In contrast, near the downstream junction corner, the tributary-mouth bar barely penetrated into the main channel (Fig. 11). This penetration may be related to the downstream flow deflection reported for the main flow corridor. The inception of the scour hole of the main channel was observed farther downstream in the experiments with $B_r = 0.30$ than in those with $B_r = 0.15$ (Fig. 11).

The sediment deposit observed along the downstream bank of the widened reach was higher and wider than the deposit that developed along the upstream bank (Figs. 11 and 12). The heights and widths of these deposits decreased as the unit-discharge ratio increased. The space between these two deposits, which corresponded to the width of the main flow corridor, increased with the increase in the unit-discharge ratio (Figs. 11 and 12). The thalweg in the main flow corridor shifted to the downstream bank of the widened reach, and its elevation increased (Fig. 12). This increase in the bed elevation was also more pronounced for higher values of the unit-discharge ratio (Figs. 8 and 12).

4. Discussion

4.1. Common hydromorphodynamic features

All experiments included common morphodynamic and hydrodynamic features that reveal a close interaction between flow dynamics and bed morphology. Specifically, these features are as follows.

- A bank-attached bar occurs along the inner bank of the main channel, downstream of the confluence. In discordant confluences in which flow recirculation may not occur (Biron et al., 1996; Best and Rhoads, 2008; Dordevic, 2012), bank-attached bars are commonly associated with zones of reduced flow velocities, in which sediment deposition is promoted by the reduced flow velocities (Biron et al., 1993, 1996; Boyer et al., 2006; Rhoads, 2006; Best and Rhoads, 2008; Guillén-Ludeña et al., 2015, 2016).
- A scour hole extends from the tributary mouth to the outer bank of the main channel, flanking the bank-attached bar. The erosion at the tributary mouth is typically related to the turbulence resulting from the flow junction, whereas the erosion along the outer bank of the main channel is associated with the flow acceleration that occurs there (Best, 1987; Bristow et al., 1993; Best and Rhoads, 2008; Rhoads et al., 2009; Guillén-Ludeña et al., 2015). This acceleration

is a consequence of the reduction of the effective flow section by the bank-attached bar and the flow deflection. The scour hole observed systematically in these experiments contrasts with the results of Biron et al. (1993), De Serres et al. (1999), and Leite Ribeiro et al. (2012a, 2012b, 2016), who associated bed discordance with the absence of marked bed erosion.
- A tributary-mouth bar whose toe barely penetrates into the main channel (Figs. 8 and 10). This bar led to a marked bed discordance between the confluent channels. This bed discordance is attributed to the abundant sediment load supplied to the tributary, which, in view of the tributary's low unit-discharge ratio ($q_r < 1$), was proportionally higher than that supplied to the main channel (Biron et al., 1993; Leite Ribeiro et al., 2012a, 2016; Guillén-Ludeña et al., 2015, 2016).

All of the hydrodynamic and morphodynamic features mentioned above are characteristic of open-channel confluences, as reported by Best (1988), Bristow et al. (1993), Boyer et al. (2006), Best and Rhoads (2008), Rhoads et al. (2009), Leite Ribeiro et al. (2012a, 2012b, 2016), and Guillén-Ludeña et al. (2015, 2016).

The results shown in this study reveal that the size of the bank-attached bar increases with the increase in the unit-discharge ratio (Table 1 and Figs. 3–6). This pattern is in agreement with the results of Best (1988) and Ghobadian and Bejestan (2007) but contrasts with the results of Leite Ribeiro et al. (2016) and Guillén-Ludeña et al. (2016), who observed a decrease in the bar size as the discharge ratio increased. This discrepancy may be explained by the different sediment mixtures used in the experiments. In this study and in the studies of Best (1988) and Ghobadian and Bejestan (2007), uniform mixtures with low gradation coefficients were used in the experiments. Conversely, the sediments used in the experiments of Leite Ribeiro et al. (2016) and Guillén-Ludeña et al. (2016) were characterized by high gradation coefficients. The size of the bank-attached bar is related to the size of the zone of reduced flow velocities on the one side and to the transport capacity of the flow over the bar on the other side. This flow corresponds to that coming from the tributary and is deflected to the inner bank of the main channel, as shown in Fig. 7. With uniform sediment, the size of the bar correlates with the size of the zone of reduced flow velocities, which increases with the discharge ratio. In contrast, with nonuniform sediments, the size of the bar appears to be somewhat associated with the transport capacity of the flow passing over the bar, which is made up of coarse particles supplied by the tributary. These particles are transported only at high discharge ratios, reducing the size of the bar with respect to those formed at low discharge ratios.

At the tributary mouth, increasing unit-discharge ratios resulted in deeper scour holes (Table 1 and Fig. 8), as reported by Best (1988), Bejestan and Hemmati (2008), Best and Rhoads (2008), and Guillén-Ludeña et al. (2016).

The bed discordance between the tributary and main channel decreased as the unit-discharge ratio increased (Fig. 8). Higher unit-discharge ratios were associated with larger flow discharges in the tributary, which had a larger transport capacity. As the supplied sediment rate was the same in all experiments, the enhanced transport capacity of the tributary flow resulted in lower bed elevations and milder bed slopes in the tributary (Guillén-Ludeña et al., 2016; Leite Ribeiro et al., 2016).

4.2. Effects of the width ratio on hydromorphodynamics

Reductions in the channel width ratio caused changes in the flow velocities in the main channel and in the tributary at equilibrium. The flow velocities in the main channel were lower for $B_r = 0.15$ than for
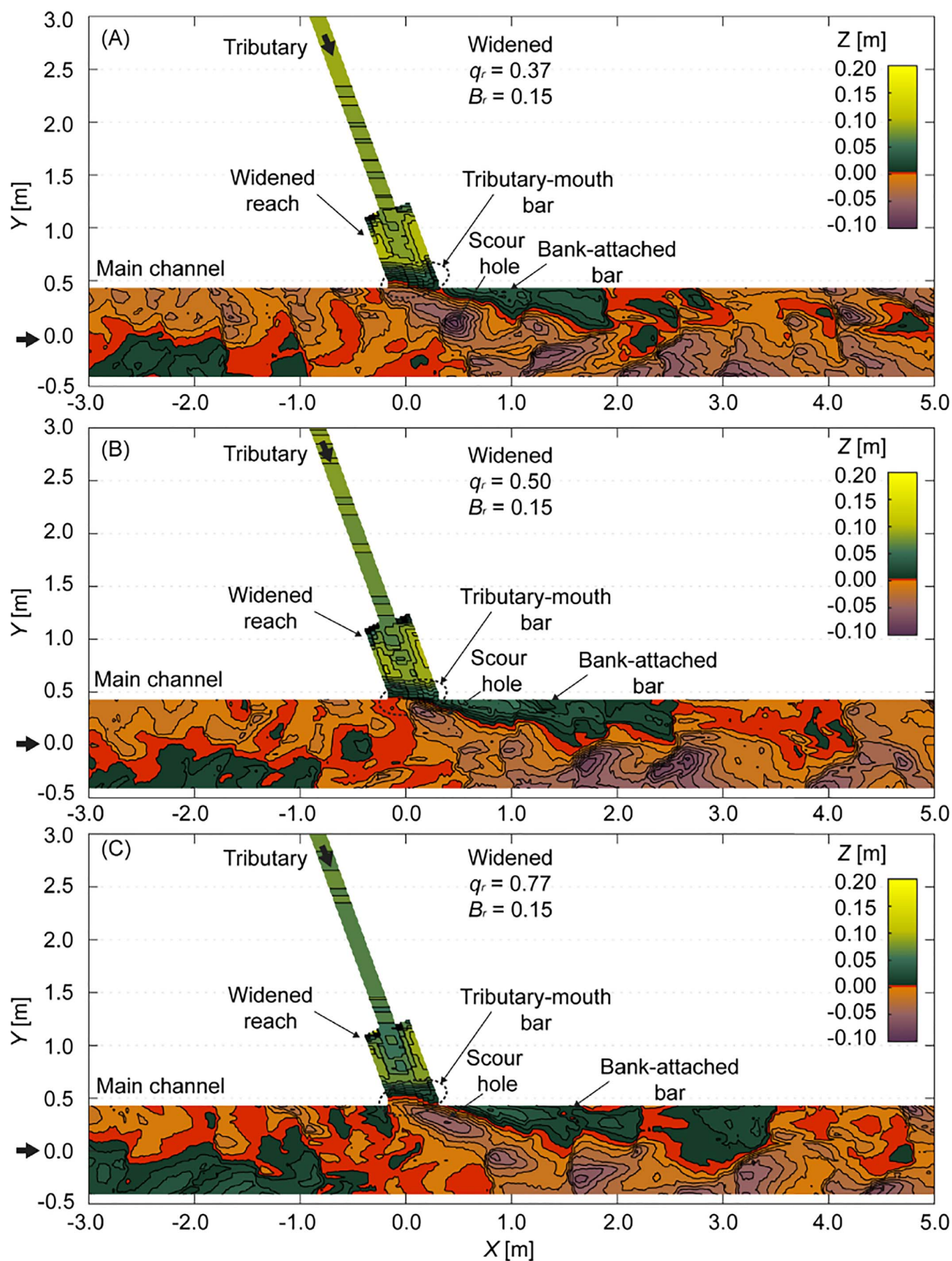
(caption on next page)

Fig. 6. Bed topography of the tributary and main channel at equilibrium for the experiments performed with B_r = 0.15 and with the widened configuration in the tributary. Each frame corresponds to a different q_r value: (A) q_r = 0.37, (B) q_r = 0.50, and (C) q_r = 0.77. The bed elevation contours are spaced by ΔZ = 0.01 m.

Table 1
Characteristic dimensions of the morphodynamic features of the main channel.

B_r	Tributary configuration	q_r	H	W	L	W/L	W/B_m	D
[−]		[−]	[m]	[m]	[m]	[−]	[−]	[m]
0.30	Reference	0.37	0.044	0.22	1.01	0.22	0.44	−0.032
		0.50	0.045	0.26	1.26	0.21	0.52	−0.060
		0.77	0.053	0.31	1.52	0.20	0.62	−0.064
	Widened	0.37	0.045	0.23	1.11	0.21	0.46	−0.043
		0.50	0.045	0.28	1.22	0.23	0.56	−0.068
		0.77	0.039	0.30	1.38	0.22	0.60	−0.056
0.15	Reference	0.37	0.059	0.63	3.32	0.19	0.63	−0.030
		0.50	0.044	0.51	2.37	0.22	0.51	−0.062
		0.77	0.049	0.71	3.03	0.23	0.71	−0.089
	Widened	0.37	0.050	0.50	2.18	0.23	0.50	−0.085
		0.50	0.052	0.50	2.23	0.22	0.50	−0.051
		0.77	0.053	0.67	3.20	0.21	0.67	−0.051

B_r = 0.30 (Table 2). Conversely, the flow velocities in the tributary were higher for B_r = 0.15 than for B_r = 0.30 (Table 3). This variation in flow velocities can be attributed to the values of unit flow discharge registered in the main channel downstream of the confluence, which differed slightly for the different width ratios. In the case of B_r = 0.30, the unit flow discharge downstream of the confluence was 0.060 m³/s/m for every unit-discharge ratio. In the case of B_r = 0.15, as the unit flow discharge supplied to the tributary and main channel upstream of the confluence were the same as those supplied for B_r = 0.30, the values of the unit flow discharge downstream of the confluence were 0.054, 0.056, and 0.057 m³/s/m for q_r = 0.37, 0.50, and 0.77 respectively. This variation in flow velocities resulted in different values of the unit momentum-flux ratio (m_r), and these values were higher for B_r = 0.15 than for B_r = 0.30 (Table 4). The unit momentum-flux ratio at equilibrium was computed as follows:

$$m_r = m_t \Big/ m_m = \frac{M_t B_m}{M_m B_t} = \frac{\rho \, Q_t U_t B_m}{\rho \, Q_m U_m B_t} \qquad (3)$$

where M stands for the momentum-flux; B is the width of each flume; Q and U denote the flow discharge and the average flow velocity upstream of the confluence at equilibrium respectively; ρ is the density of the water; and the subindexes t and m refer to the tributary and main channel respectively.

Table 4 contains the average values of the flow velocity (U), the momentum-flux (M), and the unit momentum-flux (m) of both channels measured upstream of the confluence for each experiment at equilibrium. In addition, Table 4 contains the momentum-flux ratio (M_r) and the unit momentum-flux ratio (m_r). The data contained in Table 4 show that the differences in flow velocities and in the unit momentum-flux ratio between both width ratios increase as the unit-discharge ratio increases.

In absolute terms, the increase in the width of the main channel that accompanied the change in width ratio from B_r = 0.30 to B_r = 0.15 resulted in a significantly longer and wider bank-attached bar (Table 1). During each of the experiments, the bank-attached bar grew, reducing the effective flow section and confining the flow at the outer bank, where it accelerated. The bar grew until the flow velocity at the outer bank was sufficient to erode the bar. Therefore, the increase in the size of the bar seems to be related to the width of the main channel, as a wide main channel (B_r = 0.15) would allow for a larger bar compared to a narrow main channel (B_r = 0.30).

However, in relative terms, the change in the width ratio from B_r = 0.30 to B_r = 0.15 resulted in minor differences in the ratio W/B_m, for which higher values were obtained for B_r = 0.15 than for B_r = 0.30 (Table 1). The differences observed in the ratio W/B_m for the different

width ratios may be related to the different values of the unit momentum-flux ratio corresponding to the two width ratios. According to Best and Reid (1984), the size of the zone of reduced flow velocities correlates with the momentum ratio, and according to Biron et al. (1993, 1996), Boyer et al. (2006), Rhoads (2006), Best and Rhoads (2008), and Guillén-Ludeña et al. (2015, 2016), this zone of reduced flow velocities is strongly related to the formation of the bank-attached bar. Therefore, in this study, the higher values of the unit momentum-flux ratio associated with Br = 0.15 may have led to larger zones of reduced flow velocities, which in turn resulted in relatively larger bank-attached bars with higher values of W/B_m than those obtained for Br = 0.30 (Figs. 3–6 and Table 1). The width to length ratio of the bank-attached bar (W/L in Table 1) fell within a narrow range, from 0.19 to 0.23, for all experiments. This narrow range of the width to length ratio is in good agreement with the results of Best and Reid (1984), who observed that, for a junction angle of 70°, this ratio was ~0.20.

The change from B_r = 0.30 to B_r = 0.15 also resulted in deeper scour holes at the tributary-mouth bar for the same unit-discharge ratio (Table 1 and Fig. 8). This pattern can be attributed to the higher values of the unit momentum-flux ratio associated with Br = 0.15, compared to those associated with Br = 0.30. This direct correlation between the depth of the scour hole and the momentum-flux ratio was previously reported by Best (1988) and Best and Rhoads (2008).

In the experiments performed with the widened configuration, for all of the unit-discharge ratios tested, the inception of the scour hole was observed farther downstream for a width ratio of B_r = 0.30 than for B_r = 0.15 (Fig. 11). This downstream shift can be explained by the unit momentum-flux of the main channel (m_m), which was higher for Br = 0.30 than for Br = 0.15 (Table 4). The higher momentum of the main channel associated with Br = 0.30 pushed the tributary inflow downstream, as well as the erosion associated with the flow junction.

In summary, for a given q_r value, the channel width ratio appears to be correlated with the absolute width and length of the bank-attached bar, which increase as the width ratio decreases. However, the magnitudes of other quantities, including the depth of the scour hole, the width-to-length ratio of the bank-attached bar, and the penetration of the tributary into the main channel, are instead associated with the unit-momentum-flux ratio.

4.3. Effects of the tributary configuration on hydromorphodynamics

The main differences observed in the main channel for the distinct tributary configurations are as follows.

- A recirculation zone was observed in the upstream junction corner for the widened configuration, which contrasted with the stagnation zone reported for the reference configuration (Fig. 7).
- Different heights of the bank-attached bar and different depths of the scour hole were noted in the experiments performed with equivalent unit-discharge ratios and width ratios (Table 1).
- Further penetration of the toe of the tributary-mouth bar into the main channel was noted in the experiments performed with the widened configuration (Fig. 8). The degree of penetration of the tributary-mouth bar into the main channel correlates with m_r, as this quantity had higher values in the experiments performed with the widened configuration than in those performed with the reference configuration (Table 4). Higher values of m_r indicate that the tributary was more dominant, in terms of momentum, with respect to the main channel. This greater dominance of the tributary favors the penetration of the tributary-mouth bar (Rhoads, 2006; Rhoads et al., 2009).
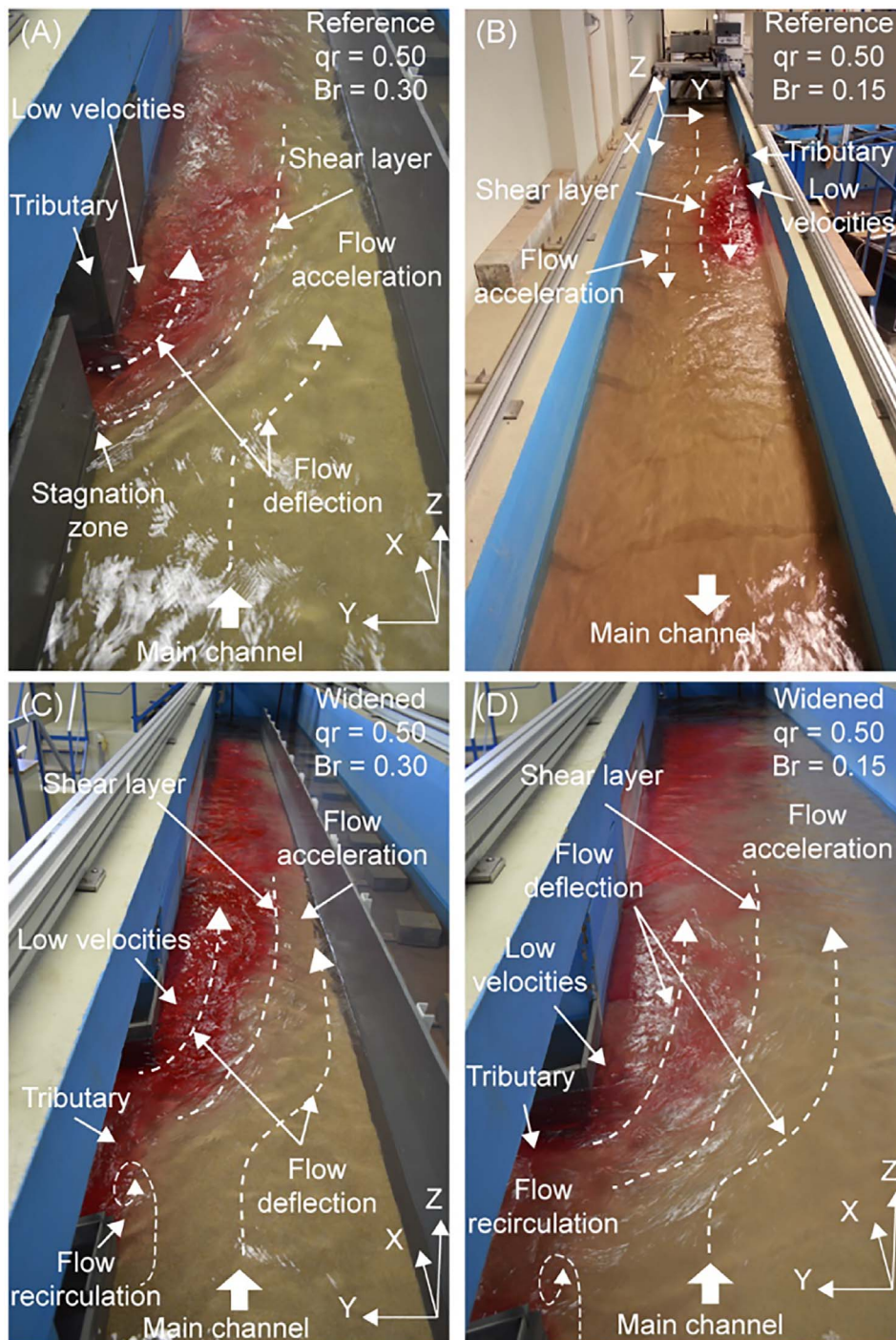
Fig. 7. View of the water surface of the main channel with dye injected in the tributary. (A) Reference configuration with $q_{r.} = 0.50$ and $B_r = 0.30$;(B) reference configuration with $q_r = 0.50$ and $B_r = 0.15$; (C) widened configuration with $q_r = 0.50$ and $B_r = 0.30$; and (D) widened configuration with $q_r = 0.50$ and $B_r = 0.15$.

With the exception of the presence of a recirculation zone at the upstream junction corner, the differences in bed morphology and flow dynamics observed in the main channel for the different tributary configurations are in agreement with the results of Leite Ribeiro et al. (2012b, 2016), who also observed variations in the size of the bank-attached bar and increased tributary penetration in experiments performed with widened tributaries. This difference may be attributed to the different junction angle, which is 70° in this study, in contrast to the 90° used in the experiments described by Leite Ribeiro et al. (2012b, 2016).

The absence of significant variations in flow depth and flow velocities in the main channel for the different tributary configurations was also reported by Leite Ribeiro et al. (2012b, 2016).

In the tributary and upstream of the widened reach ($Y > 1.2$ m),

no significant differences were observed in the bed morphology for the distinct tributary configurations (Fig. 8). However, in terms of hydrodynamics, the experiments performed with the widened configuration yielded lower flow depths and higher velocities, and thus higher Froude numbers, than those performed with the reference configuration. This difference may be attributed to the different downstream boundary conditions of the tributary. These boundary conditions consisted of (i) the widened reach in the case of the experiments performed with the widened configuration, and (ii) the main channel in the case of the experiments performed with the reference configuration. These results contrast with the results of Leite Ribeiro et al. (2012b, 2016), in which no differences in flow depth were observed in the tributary for the different tributary configurations. The differences between this study and those by Leite Ribeiro et al. (2012b, 2016) may be related to the

Table 2
Average values of flow depth (h), flow velocity (U), and the Froude number (Fr) as measured in the main channel upstream and downstream of the confluence (subindexes *up* and *dw* respectively).

B_r	Tributary configuration	q_r	h_{up}	U_{up}	Fr_{up}	h_{dw}	U_{dw}	Fr_{dw}
[−]		[−]	[m]	[m/s]	[−]	[m]	[m/s]	[−]
0.30	Reference	0.37	0.122	0.444	0.41	0.116	0.516	0.48
		0.50	0.113	0.462	0.44	0.114	0.528	0.50
		0.77	0.103	0.473	0.47	0.116	0.516	0.48
	Widened	0.37	0.117	0.463	0.43	0.115	0.520	0.49
		0.50	0.116	0.452	0.42	0.120	0.500	0.46
		0.77	0.105	0.464	0.46	0.115	0.521	0.49
0.15	Reference	0.37	0.126	0.429	0.39	0.130	0.437	0.39
		0.50	0.116	0.451	0.42	0.114	0.493	0.47
		0.77	0.116	0.422	0.40	0.114	0.477	0.45
	Widened	0.37	0.127	0.427	0.38	0.125	0.457	0.41
		0.50	0.124	0.421	0.38	0.125	0.451	0.41
		0.77	0.114	0.428	0.40	0.116	0.469	0.44

Table 3
Average flow depth (h), average flow velocity (U), and average Froude number (Fr) measured in the tributary, where $Y > 1.0$ m for the reference configuration and $Y > 1.2$ m for the widened configuration.

B_r	Tributary configuration	q_r	H	U	Fr
[−]		[−]	[m]	[m/s]	[−]
0.30	Reference	0.37	0.044	0.455	0.69
		0.50	0.050	0.520	0.74
		0.77	0.069	0.541	0.66
	Widened	0.37	0.039	0.519	0.85
		0.50	0.046	0.568	0.85
		0.77	0.061	0.611	0.79
0.15	Reference	0.37	0.041	0.488	0.77
		0.50	0.049	0.531	0.77
		0.77	0.065	0.574	0.72
	Widened	0.37	0.038	0.526	0.86
		0.50	0.045	0.575	0.86
		0.77	0.058	0.639	0.84

tributary flow regime, which was critical or supercritical ($Fr \geq 1$) in the case of Leite Ribeiro et al. (2012b, 2016) and subcritical ($Fr < 1$) for all experiments performed in this study. The flow regime of the tributary at equilibrium corresponded to the hydromorphodynamic response to the imposed flow and sediment supply rates, as reported by Guillén-Ludeña et al. (2016). In the case of Leite Ribeiro et al. (2012b, 2016), in which the confluence angle was 90°, and the sediment mixture was composed of a wide range of particle sizes, the tributary evolved to a supercritical flow regime to convey the imposed sediment load to the main channel. In this study, the delivery of the tributary sediment load into the main channel was facilitated by the lower confluence angle (70°) and the uniform sediment mixture used, which resulted in a subcritical flow regime in the tributary.

The hydromorphodynamics of the widened reach displayed features similar to those reported by Leite Ribeiro et al. (2012b, 2016). These features were as follows.

- A main flow corridor characterized by larger flow depths and high flow velocity was noted (Fig. 12). This corridor was deflected toward the downstream bank of the widened reach by the influence of the main channel. In this corridor, the bed elevation increased close to the confluence. Leite Ribeiro et al. (2012b, 2016) attributed this raise in level to flow expansion within the widened reach. However, in this study, flow expansion was less noticeable than in the case of Leite Ribeiro et al. (2012b, 2016), probably because of the different flow regimes that were present in the tributaries in the two experiments and to the smaller junction angle used in this study.
- Two recirculation zones occurred along either bank of the widened
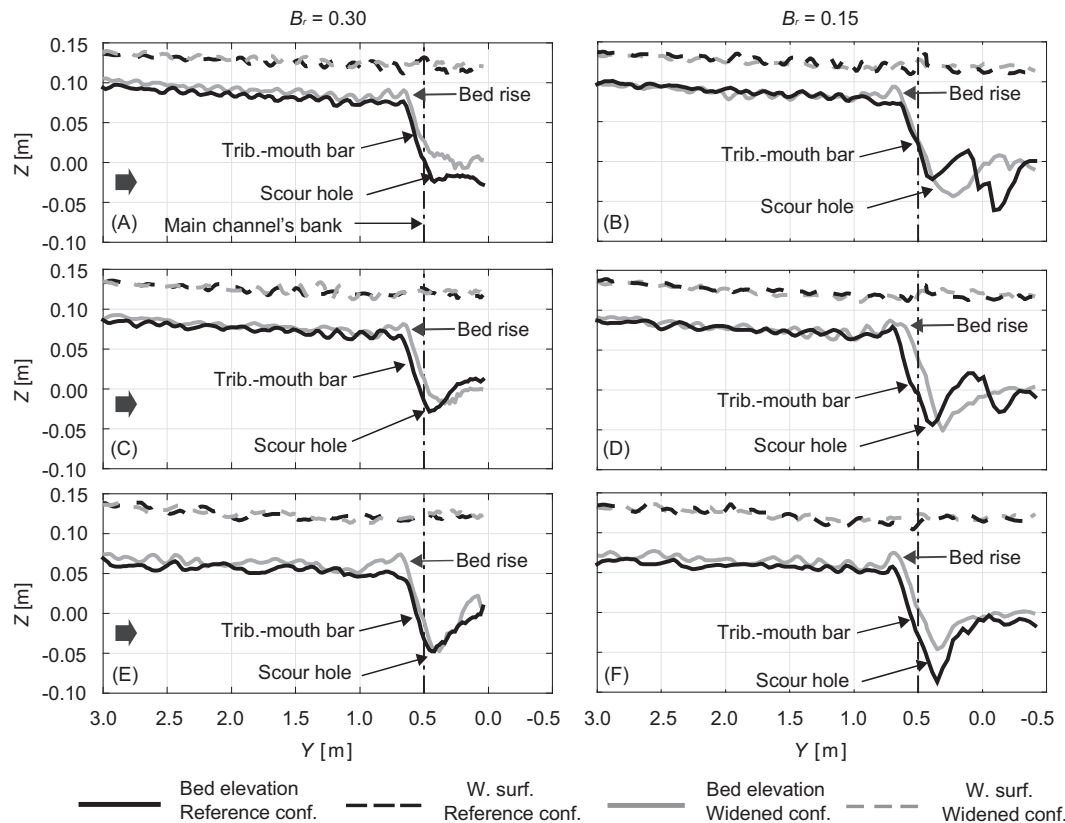
Fig. 8. Bed elevation and water surface profiles along the tributary axis. Each plot depicts the results for both tributary configurations (reference and widened). (A) $q_r = 0.37$ and $Br = 0.30$, (B) $q_r = 0.37$ and $Br = 0.15$, (C) $q_r = 0.50$ and $Br = 0.30$, (D) $q_r = 0.50$ and $Br = 0.15$, (E) $q_r = 0.77$ and $Br = 0.30$, and (F) $q_r = 0.77$ and $Br = 0.15$.
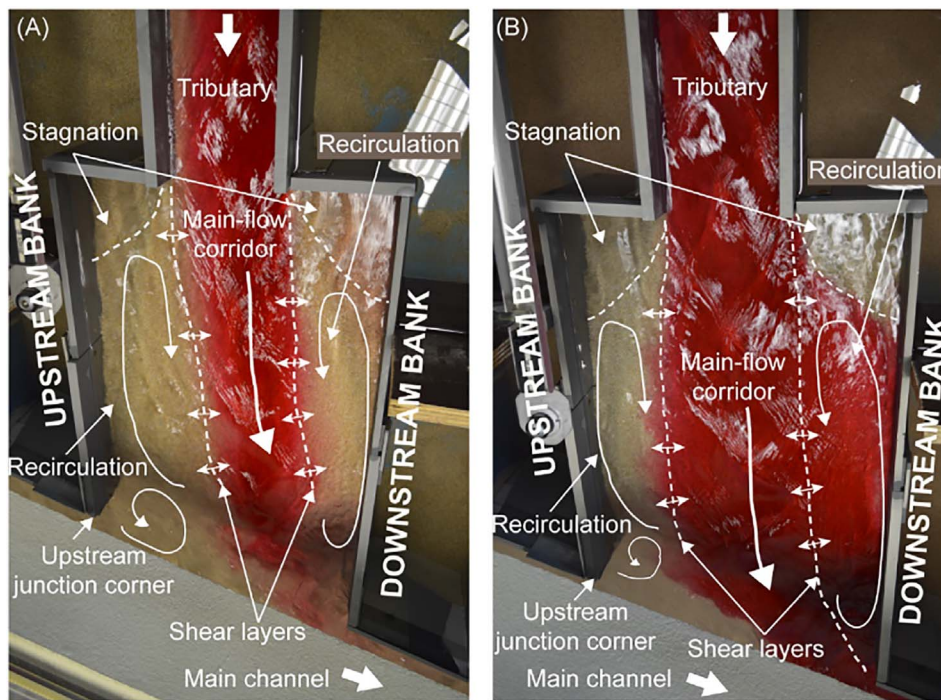
Fig. 9. Planview of the widened reach for $q_r = 0.37$ and $B_r = 0.30$ at two consecutive instants (A and B) when dye was injected upstream into the tributary.
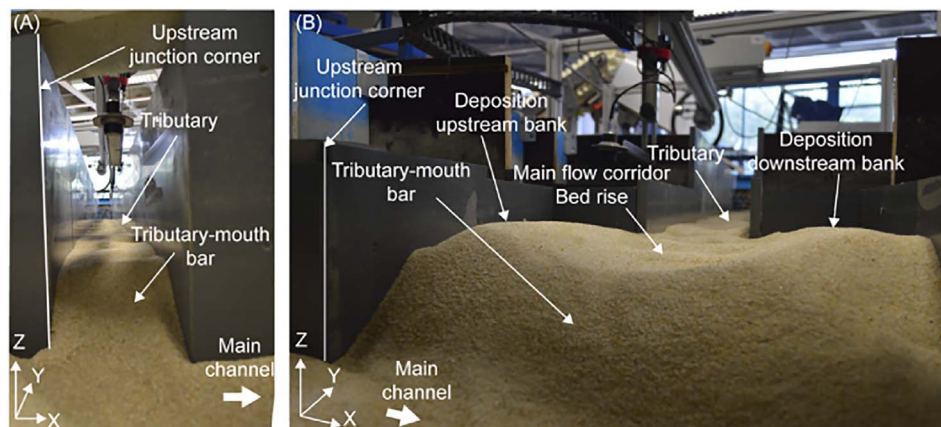

Fig. 10. View of the final topography from the tributary mouth corresponding to $q_r = 0.37$ and $B_r = 0.30$ for (A) the reference configuration and (B) the widened configuration.

reach that flanked the main flow corridor. These zones were characterized by low flow depths and reduced flow velocities (Fig. 12). These zones correspond to the stagnation zones reported by Leite Ribeiro et al. (2012b, 2016), in which flow recirculation was also observed. In these zones, the low flow velocity resulted in sediment deposition, as shown in Figs. 10–12. As observed by Leite Ribeiro et al. (2012b, 2016), the recirculation zone located along the upstream bank of the widened reach was mainly fed by the main channel flow, whereas that located along the downstream bank was fed by the tributary flow (Fig. 9). This sedimentation pattern differs from that reported by Leite Ribeiro et al. (2012b, 2016), who observed no sediment deposition along the upstream bank of the widened reach because they did not supply the main channel with sediment during the experiments. Hence, the absence of sediment supply to the main channel resulted in no deposition along the upstream bank of the widened reach. Conversely, the main channel was fed with sediments in this study, which resulted in sediment deposition within the recirculation zone.

In summary, local tributary widening enhances the heterogeneity in

flow depths and flow velocities at confluences when compared to the reference configuration. Additionally, the effects of the local tributary widening on flow dynamics and bed morphology are limited to the widened reach, and the widening has minor or negligible effects on the main channel. This outcome is favorable for flood safety reasons. These findings reinforce the suitability of local tributary widening as a potential solution for the rehabilitation of river confluences.

5. Conclusions

The influence of the width ratio and local tributary widening on the hydrodynamics and morphodynamics of the confluence were analyzed by means of 12 laboratory experiments. Three unit-discharge ratios ($q_r = 0.37$, 0.50, and 0.77) and two width ratios ($B_r = 0.15$ and 0.30) were tested using two tributary configurations (widened and reference). The different width ratios were obtained by changing the width of the main channel. The tributary configurations consisted of (i) a straight rectangular tributary with constant width (reference configuration), and (ii) a straight rectangular tributary with a local widening at the downstream reach (widened configuration). In general, the results
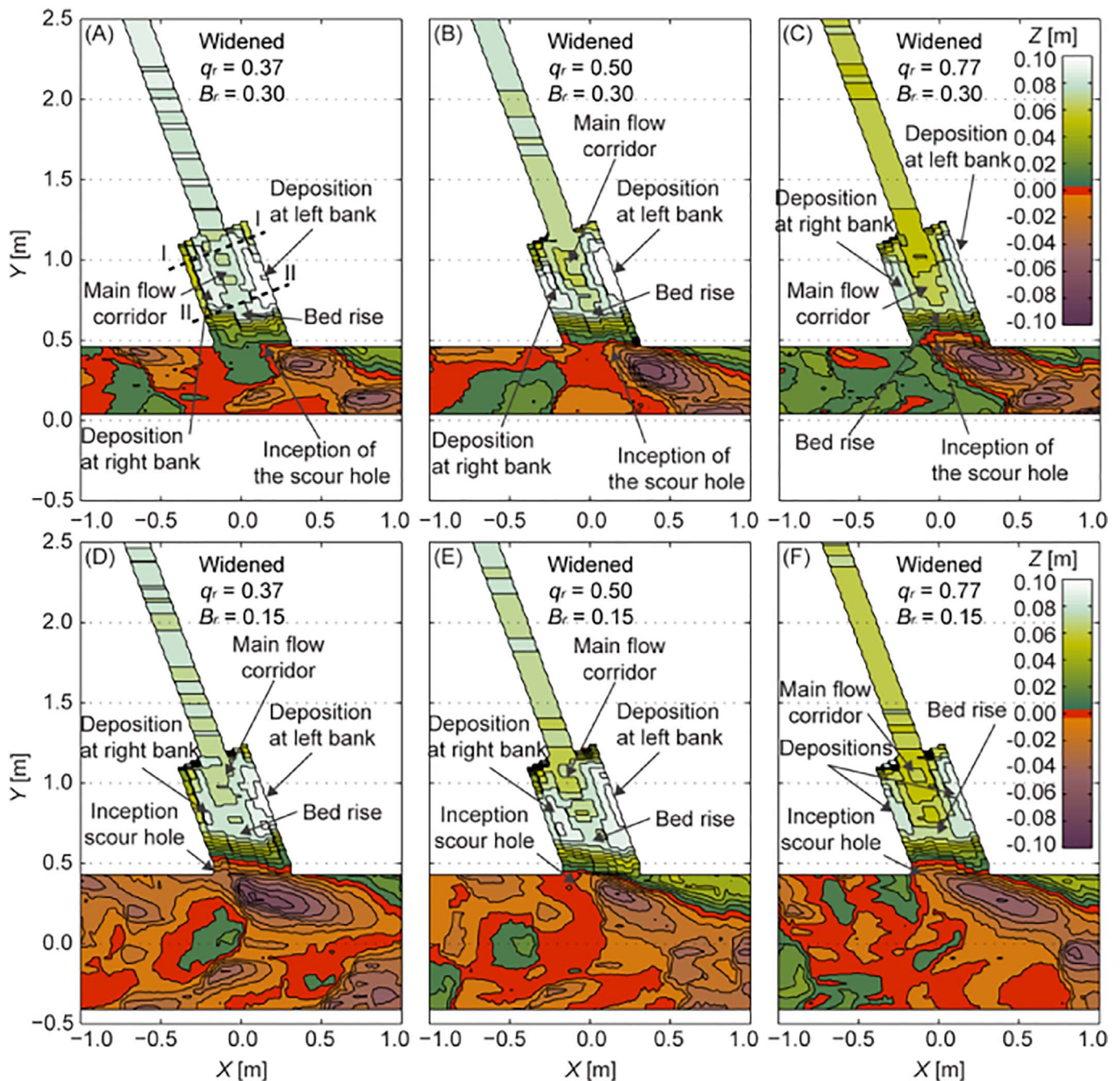
Fig. 11. Detailed planview of the bed topography at the confluence for the experiments performed with the widened configuration.

showed a close interaction between bed morphology and flow dynamics.

The effects of the channel width ratio were primarily observed in the main channel, with negligible effects on the tributary. Although the bed morphology obtained for $Br = 0.15$ included larger bank-attached bars, deeper scour holes, and farther penetration of the tributary-mouth into the main channel than that obtained for $Br = 0.30$, the width ratio seems to be responsible only for the changes in the absolute dimensions (i.e., width and length) of the bank-attached bar. The rest of the morphological differences were attributed to the different values of the unit momentum-flux ratio (m_r) at equilibrium, which were larger for $Br = 0.15$ than for $Br = 0.30$. The different unit momentum-flux ratios at equilibrium result from slight variations in the unit flow discharge downstream of the confluence in the different experiments.

The effects of the local tributary widening on the hydro-morphodynamics of the confluence were mainly observed within the widened reach of the tributary, where the flow dynamics and bed morphology were characterized by heterogeneity in flow depths and flow velocities. This heterogeneity contrasted with the homogeneity in flow depth and flow velocity observed in the tributary for the experiments performed with the reference configuration. In contrast to previously reported results, the local tributary widening also influenced the flow dynamics of the upstream reach of the tributary. Here, the flow regime was characterized by higher Froude numbers, compared to those in the experiments performed with the reference configuration. In the main channel, only minor differences were observed in the flow dynamics and bed morphology for the distinct tributary configurations.
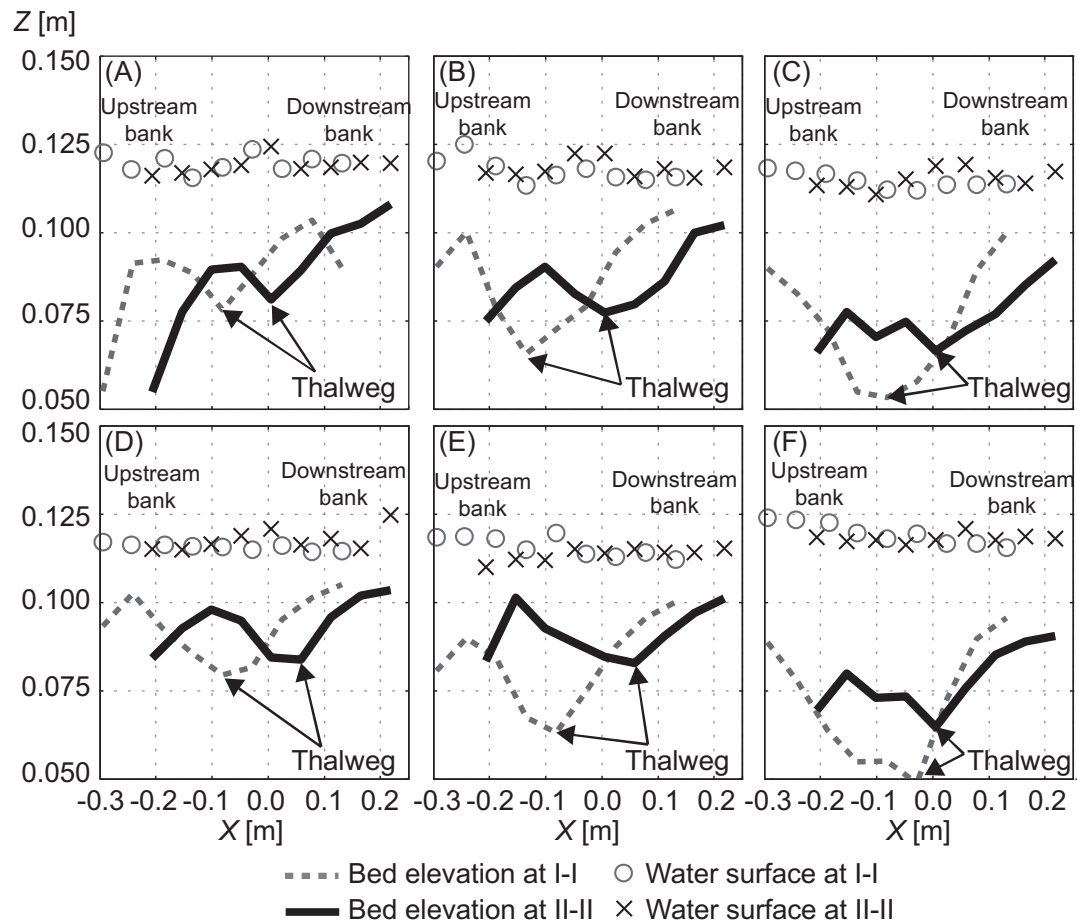
Fig. 12. Bed elevation and water surface of the widened reach at sections I-I and II-II defined in Fig. 11A for (A) $q_r = 0.37$ and $B_r = 0.30$, (B) $q_r = 0.50$ and $B_r = 0.30$, (C) $q_r = 0.77$ and $B_r = 0.30$, (D) $q_r = 0.37$ and $B_r = 0.15$, (E) $q_r = 0.50$ and $B_r = 0.15$, and (F) $q_r = 0.77$ and $B_r = 0.15$.

Table 4
Values of the average flow velocity (U) measured upstream of the confluence for both channels, the momentum-flux for the tributary and main channel (M_t and M_m respectively), the unit momentum-flux for the tributary and main channel (m_t and m_m respectively), the momentum-flux ratio (M_r), and the unit momentum-flux ratio (m_r).

B_r	Tributary configuration	q_r	U_t	M_t	m_t	U_m	M_m	m_m	M_r	m_r
[−]		[−]	[m/s]	[N]	[N/m]	[m/s]	[N]	[N/m]	[−]	[−]
0.30	Reference	0.37	0.455	1.36	9.09	0.444	12.00	24.00	0.11	0.38
		0.50	0.520	2.03	13.52	0.462	12.07	24.13	0.17	0.56
		0.77	0.541	3.03	20.20	0.473	11.54	23.08	0.26	0.88
	Widened	0.37	0.519	1.56	10.39	0.463	12.50	25.01	0.12	0.42
		0.50	0.568	2.21	14.76	0.452	11.79	23.57	0.19	0.63
		0.77	0.611	3.42	22.81	0.464	11.33	22.66	0.30	1.01
0.15	Reference	0.37	0.488	1.46	9.76	0.429	23.16	23.16	0.06	0.42
		0.50	0.531	2.07	13.80	0.451	23.53	23.53	0.09	0.59
		0.77	0.574	3.22	21.44	0.422	20.58	20.58	0.16	1.04
	Widened	0.37	0.526	1.58	10.53	0.427	23.03	23.03	0.07	0.46
		0.50	0.575	2.24	14.96	0.421	21.97	21.97	0.10	0.68
		0.77	0.639	3.58	23.87	0.428	20.87	20.87	0.17	1.14

References

Bejestan, M.S., Hemmati, M., 2008. Scour depth at river confluence of unequal bed level. J. Appl. Sci. 8 (9), 1766-1760. http://dx.doi.org/10.3923/jas.2008.1766.1770.

Benda, L., Poff, N.L., Miller, D., Dunne, T., Reeves, G., Pess, G., Pollock, M., 2004. The Network dynamics hypothesis: how channel networks structure riverine habitats. Bioscience 54 (5), 413. http://dx.doi.org/10.1641/0006-3568(2004)054[0413:TNDHHC]2.0.CO;2.

Bernhardt, E.S., 2005. Synthesizing U.S. river restoration efforts. Science 308 (5722), 636–637. http://dx.doi.org/10.1126/science.1109769.

Bernhardt, E.S., Sudduth, E.B., Palmer, M.A., Allan, J.D., Meyer, J.L., Alexander, G., Pagano, L., 2007. Restoring rivers one reach at a time: results from a survey of U.S. river restoration practitioners. Restor. Ecol. 15 (3), 482–493. http://dx.doi.org/10.1111/j.1526-100X.2007.00244.x.

Best, J.L., 1987. Flow dynamics at river channel confluences: implications for sediment transport and bed morphology. Recent developments in fluvial sedimentology. Spec. Publ. SEPM Soc. Sediment. Geol. (39), 27–35. http://dx.doi.org/10.2110/pec.87.39.0027.

Best, J.L., 1988. Sediment transport and bed morphology at river channel confluences. Sedimentology 35 (3), 481–498. http://dx.doi.org/10.1111/j.1365-3091.1988.tb00999.x.

Best, J.L., Reid, I., 1984. Separation zone at open-channel junctions. J. Hydraul. Eng. 110 (11), 1588–1594. http://dx.doi.org/10.1061/(ASCE)0733-9429(1984)110:11(1588).

Best, J.L., Rhoads, B.L., 2008. Sediment transport, bed morphology and the sedimentology of river channel confluences. In: River Confluences, Tributaries and the Fluvial Network. John Wiley & Sons, Ltd., pp. 45–72. http://dx.doi.org/10.1002/9780470760383.ch4.

Biron, P., Roy, A., Best, J.L., Boyer, C.J., 1993. Bed morphology and sedimentology at the confluence of unequal depth channels. Geomorphology 8 (2–3), 115–129. http://dx.doi.org/10.1016/0169-555x(93)90032-w.

Biron, P., Best, J.L., Roy, A.G., 1996. Effects of bed discordance on flow dynamics at open channel confluences. J. Hydraul. Eng. 122 (12), 676–682. http://dx.doi.org/10.1061/(ASCE)0733-9429(1996)122:12(676).

Boyer, C., Roy, A.G., Best, J.L., 2006. Dynamics of a river channel confluence with discordant beds: flow turbulence, bed load sediment transport, and bed morphology. J. Geophys. Res. 111 (F4), F04007. http://dx.doi.org/10.1029/2005jf000458.

Bristow, C.S., Best, J.L., Roy, A.G., 1993. Morphology and facies models of channel confluences. In: Marzo, M., Puigdefábregas, C. (Eds.), Alluvial Sedimentation, pp. 91–100. (Ltd, Oxford, Uk). http://dx.doi.org/10.1002/9781444303995.ch8.

De Serres, B., Roy, A.G., Biron, P.M., Best, J.L., 1999. Three-dimensional structure of flow at a confluence of river channels with discordant beds. Geomorphology 26 (4), 313–335. http://dx.doi.org/10.1016/S0169-555X(98)00064-6.

Dordevic, D., 2012. Role of bed elevation discordance at 90o straight-channel confluences. In: Proceedings of 6th Int. Conference on Fluvial Hydraulics - River Flow. 2. pp. 1153–1160.

Fette, M., Weber, C., Peter, A., Wehrli, B., 2007. Hydropower production and river rehabilitation: a case study on an alpine river. Environ. Model. Assess. 12 (4), 257–267. http://dx.doi.org/10.1007/s10666-006-9061-7.

Ghobadian, R., Bejestan, M.S., 2007. Investigation of sediment patterns at river confluence. J. Appl. Sci. 7 (10), 1372–1380. http://dx.doi.org/10.3923/jas.2007.1372.1380.

Guillén Ludeña, S., Cheng, Z., Constantinescu, G., Franca, M.J., 2017. Hydrodynamics of mountain-river confluences and its relationship to sediment transport. J. Geophys. Res. Earth Surf. http://dx.doi.org/10.1002/2016JF004122.

Guillén-Ludeña, S., 2015. Hydro-morphodynamics of open-channel confluences with low discharge ratio and dominant tributary sediment supply. In: Ecole Polytechnique Fédérale de Lausanne, Lausanne, Switzerland. Lausanne, EPFL.

Guillén-Ludeña, S., Franca, M.J., Cardoso, A.H., Schleiss, A.J., 2015. Hydro-morphodynamic evolution in a 90° movable bed discordant confluence with low discharge ratio. Earth Surf. Process. Landf. 40 (14), 1927–1938. http://dx.doi.org/10.1002/esp.3770.

Guillén-Ludeña, S., Franca, M.J., Cardoso, A.H., Schleiss, A.J., 2016. Evolution of the hydromorphodynamics of mountain river confluences for varying discharge ratios and junction angles. Geomorphology 255, 1–15. http://dx.doi.org/10.1016/j.geomorph.2015.12.006.

Leite Ribeiro, M., Blanckaert, K., Roy, A.G., Schleiss, A.J., 2012a. Flow and sediment dynamics in channel confluences. J. Geophys. Res. Earth Surf. 117 (F1), 1–19. http://dx.doi.org/10.1029/2011JF002171.

Leite Ribeiro, M., Blanckaert, K., Roy, A.G., Schleiss, A.J., 2012b. Hydromorphological implications of local tributary widening for river rehabilitation. Water Resour. Res. 48 (10) (n/a-n/a). http://dx.doi.org/10.1029/2011WR011296.

Leite Ribeiro, M., Blanckaert, K., Schleiss, A.J., 2016. Local tributary widening for river rehabilitation. Ecohydrology 9 (2), 204–217. http://dx.doi.org/10.1002/eco.1588.

Mosley, M.P., 1976. An experimental study of channel confluences. J. Geol. 84 (5), 535–562. (Retrieved from). http://www.jstor.org/stable/30066212.

Moyle, P.B., Mount, J.F., 2007. Homogenous rivers, homogenous faunas. Proc. Natl. Acad. Sci. 104 (14), 5711–5712. http://dx.doi.org/10.1073/pnas.0701457104.

Nakamura, K., Tockner, K., Amano, K., 2006. River and wetland restoration: lessons from Japan. Bioscience 56 (5), 419. http://dx.doi.org/10.1641/0006-3568(2006)056[0419:RAWRLF]2.0.CO;2.

Palmer, M.A., Menninger, H.L., Bernhardt, E.S., 2010. River restoration, habitat heterogeneity and biodiversity: a failure of theory or practice? Freshw. Biol. 55, 205–222. http://dx.doi.org/10.1111/j.1365-2427.2009.02372.x.

Peter, A., 2006. Rehabilitation – to What Extent, and Why? Eawag News, 61e(November). pp. 4–8.

Reichert, P., Borsuk, M., Hostmann, M., Schweizer, S., Spörri, C., Tockner, K., Truffer, B., 2007. Concepts of decision support for river rehabilitation. Environ. Model Softw. 22 (2), 188–201. http://dx.doi.org/10.1016/j.envsoft.2005.07.017.

Rhoads, B.L., 2006. Scaling of confluence dynamics in river systems: some general considerations. In: Parker, G., Garcia, M. (Eds.), River, Coastal and Estuarine Morphodynamics. Taylor and Francis, London, pp. 379–387.

Rhoads, B.L., Riley, J.D., Mayer, D.R., 2009. Response of bed morphology and bed material texture to hydrological conditions at an asymmetrical stream confluence. Geomorphology 109 (3–4), 161–173. http://dx.doi.org/10.1016/j.geomorph.2009.02.029.

Rice, S.P., Ferguson, R.I., Hoey, T.B., 2006. Tributary control of physical heterogeneity and biological diversity at river confluences. Can. J. Fish. Aquat. Sci. 63 (11), 2553–2566. http://dx.doi.org/10.1139/f06-145.

Rice, S.P., Kiffney, P., Pess, G.R., 2008. The ecological importance of tributaries and confluences. In: Rice, S.P., Roy, A.G., Rhoads, B.L. (Eds.), River Confluences, Tributaries and the Fluvial Network. John Wiley & Sons, Ltd., New York, pp. 209–242.

Sloff, C., Havinga, H., Jagers, H., 2006. Knowledge requirements for sustainable fairway management. In: Parker, G., García, M. (Eds.), Proceedings of the 4th IAHR Symposium on River, Coastal and Estuarine Morphodynamics (RCEM 2005). Taylor & Francis, Urbana, Illinois, USA. http://dx.doi.org/10.1201/9781439833896.ch127.

Smart, G.M., 1984. Sediment transport formula for steep channels. J. Hydraul. Eng. 110 (3), 267–276. http://dx.doi.org/10.1061/(ASCE)0733-9429(1984)110:3(267).

Weber, C., Schager, E., Peter, A., 2009. Habitat diversity and fish assemblage structure in local river widenings: a case study on a Swiss river. River Res. Appl. 25 (6), 687–701. http://dx.doi.org/10.1002/rra.1176.